The Modeling of Singularities in the Finite-Difference Approximation of the Time-Domain Electromagnetic-Field Equations

GERRIT MUR

Abstract—**When the electromagnetic-field equations are solved in a region with a corner, singularities in the field or in its spatial derivatives will be present at these corners. These singularities cause the local truncation error in a finite-difference approximation of the field equations to be unbounded. In this paper it is shown that failing to take these singularities into account leads to large errors in the finite-difference solution of the time-domain electromagnetic-field equations. A simple method is described to account for these singularities while retaining the simplicity of the finite-difference formulation. Numerical results are given that demonstrate the accuracy obtained when our technique is used.**

I. Introduction

RECENTLY, the finite-difference formulation of time-domain electromagnetic-field problems has been used for solving a wide variety of field problems [1]–[7]. For these problems, finite-difference methods have the advantage of being efficient and very flexible. When the configuration under investigation contains a conducting obstacle with edges, which is often the case, the domain in which the field has to be computed will usually have corners. At a corner the field, or one of its spatial derivatives, has a singularity which would cause the local truncation error in the finite-difference approximation of the field-equations to be unbounded. Consequently, the error in the numerical solution of the field problem could be large when singularities are not taken into account. In this paper we present a method to account for these singularities while retaining the simplicity of the finite-difference formulation. The method is described and tested for two-dimensional configurations and for fields that are either E- or H-polarized. It can also, in principle, be used for three-dimensional configurations. Numerical results are presented to demonstrate that for accurate results to be obtained the singularities must be taken into account.

II. Finite-Difference Approximations of the Electromagnetic-Field Equations

In Fig. 1 we have depicted a cross section of the two-dimensional configuration to be investigated. The configuration is uniform in the z-direction of a Cartesian coordinate system and we assume that the fields in the configuration do not depend on z. The region that is occupied by the perfectly conducting obstacle is indicated as S_C. It has a boundary C and the region surrounding the conductor is S. Since the behavior of the field near the edges of S_C does not depend on the properties of the homogeneous medium in S but only on the angle α (see Fig. 1) we can, without restricting ourselves, assume that the properties of the medium in S are those of a vacuum. For fields that do not depend on z, the electromagnetic-field equations reduce to two uncoupled sets of three equations, namely one for the case of E-polarization, i.e., when $\boldsymbol{E}=E_z\boldsymbol{i}_z$

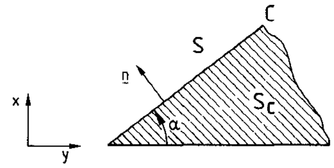

Fig. 1. Cross section of a perfectly conducting obstacle that is uniform in the z-direction.

$$\mu_0\partial_t H_x = -\partial_y E_z \tag{1a}$$

$$\mu_0\partial_t H_y = \partial_x E_z \tag{1b}$$

$$\epsilon_0\partial_t E_z = \partial_x H_y - \partial_y H_x \tag{1c}$$

and one for the case of H-polarization, i.e., when $\boldsymbol{H}=H_z\boldsymbol{i}_z$

$$\epsilon_0\partial_t E_x = \partial_y H_z \tag{2a}$$

$$\epsilon_0\partial_t E_y = -\partial_x H_z \tag{2b}$$

$$\mu_0\partial_t H_z = \partial_y E_x - \partial_x E_y. \tag{2c}$$

For both cases we have the boundary condition

$$\boldsymbol{n}\times\boldsymbol{E}=\boldsymbol{0}, \qquad \text{on } C \tag{3}$$

where $\boldsymbol{n}$ denotes the unit vector along the normal to C. We now introduce the finite-difference approximation of (1) and (2) and write any function of space and time as

$$F^n(i,j)=F(ih,jh,nk) \tag{4}$$

where $h=\delta x=\delta y$ is the space increment and $k=\delta t$ is the time increment. By positioning the field components of $\boldsymbol{E}$ and $\boldsymbol{H}$ on the mesh in the way that is depicted in Fig. 2 and evaluating the relevant components of $\boldsymbol{E}$ and $\boldsymbol{H}$ at alternate half-time steps we obtain finite-difference expressions that

Manuscript received March 23, 1981; revised June 3, 1981.

The author is with the Department of Electrical Engineering, Laboratory of Electromagnetic Research, Delft University of Technology, P.O. Box 5031 2600 GA Delft, The Netherlands.

0018-9480/81/1000-1073$00.75

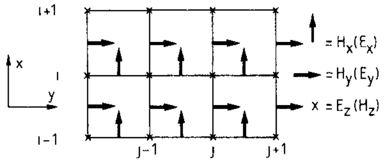

Fig. 2. Positions of the field components on the mesh for E-polarization (H-polarization).

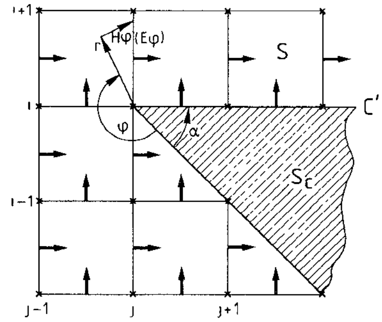

Fig. 3. The approximated boundary C' and a local polar coordinate system centered at the corner at node (i, j).

have a local truncation error of the second order in all increments. The finite-difference approximation for (1) is

$$H_x^{n+1/2}(i, j+1/2)=H_x^{n-1/2}(i, j+1/2) -(k/\mu_0 h)\left(E_z^n(i, j+1)-E_z^n(i, j)\right) \quad (5a)$$

$$H_y^{n+1/2}(i+1/2, j)=H_y^{n-1/2}(i+1/2, j) +(k/\mu_0 h)\left(E_z^n(i+1, j)-E_z^n(i, j)\right) \quad (5b)$$

$$E_z^{n+1}(i, j)=E_z^n(i, j)+(k/\epsilon_0 h)\left(H_y^{n+1/2}(i+1/2, j) -H_y^{n+1/2}(i-1/2, j)-H_x^{n+1/2}(i, j+1/2) +H_x^{n+1/2}(i, j-1/2)\right). \quad (5c)$$

The finite-difference approximation for (2) is

$$E_x^{n+1/2}(i, j+1/2)=E_x^{n-1/2}(i, j+1/2) +(k/\epsilon_0 h)\left(H_z^n(i, j+1)-H_z^n(i, j)\right) \quad (6a)$$

$$E_y^{n+1/2}(i+1/2, j)=E_y^{n-1/2}(i+1/2, j) -(k/\epsilon_0 h)\left(H_z^n(i+1, j)-H_z^n(i, j)\right) \quad (6b)$$

$$H_z^{n+1}(i, j)=H_z^n(i, j)+(k/\mu_0 h)\left(E_x^{n+1/2}(i, j+1/2) -E_x^{n+1/2}(i, j-1/2)-E_y^{n+1/2}(i+1/2, j) +E_y^{n+1/2}(i-1/2, j)\right). \quad (6c)$$

We note that (5) and (6) are a two-dimensional form of Yee's algorithm [1]. The condition for stability of (5) and (6) is [3]

$$k \leq h/\left(c_0\sqrt{2}\right) \quad (7)$$

where $c_0=(\epsilon_0\mu_0)^{-1/2}$ denotes the speed of light *in vacuo*. It can easily be shown that (5) and (6) have a local truncation error of the second order in all increments.

As to the approximation of the boundary C of the obstacle we note that C will usually not coincide with the lines through the nodes of the mesh. It is, in principle, possible to derive finite-difference approximations of the boundary conditions for an arbitrary C. This, however, would yield complicated difference equations and would require a large amount of logic. In order to circumvent these problems we introduce an approximated boundary C' that passes through the nodes (i, j), with i, j integer, and that consists of straight lines which are either parallel to the x- or y-axis or are at an angle of $\pi/4$ with the coordinate directions (see Fig. 3). The nodes through which C' passes are chosen such that the closest possible fit is obtained and the error in the location of C' made in this way is always less than $h/2$.

III. Approximations for Edge Singularities

In this section we shall deal with the approximation of the field near a corner in the configuration, i.e., in a region where a component of the field, or a spatial derivative of such a component, may be singular, thus making the error in (5) and (6) applied to such a region to be unbounded. We shall start with the case of E-polarization.

A. Edge Singularities, E-Polarization

In the case of E-polarization C' passes through the E_z-nodes. From (3) it follows that $E_z=0$ on C', even for nodes on the edge of a corner. For the H_x and H_y nodes that are at a distance $h/2$ from such an edge (5a) and (5b) cannot be used since E_z is not differentiable near the edge and consequently the error in (5a) and (5b) would be unbounded. To overcome this difficulty we now analyze the field near a corner by introducing a local polar coordinate system (see Fig. 3). For E_z and H_φ we have

$$\mu_0\partial_t H_\varphi(r, \varphi, t)=\partial_r E_z(r, \varphi, t). \quad (8)$$

Near the edge E_z and H_φ can, by using the expansion given by Jones [8], be approximated as

$$E_z=c_1(t)r^{\nu_1}\sin(\nu_1\varphi)+c_2(t)r^{\nu_2}\sin(\nu_2\varphi)+\cdots \quad (9)$$

$$H_\varphi=c_1(t)Y_1(t)r^{\nu_1-1}\sin(\nu_1\varphi) +c_2(t)Y_2(t)r^{\nu_2-1}\sin(\nu_2\varphi)+\cdots \quad (10)$$

with

$$\nu_n=n\pi/(2\pi-\alpha). \quad (11)$$

We now apply (8) to a point at a distance $h/2$ from the edge. Using the leading term of (9) in (8) we obtain

$$\mu_0\partial_t H_\varphi(h/2, \varphi, t)=\left(\partial_r E_z(r, \varphi, t)\right)\big|_{r=h/2} =\nu_1 2^{1-\nu_1}E_z(h, \varphi, t)/h. \quad (12)$$

Using the central difference approximation for the time derivative we obtain from (12)

$$H_\varphi(h/2, \varphi, (n+1/2)k)=H_\varphi(h/2, \varphi, (n-1/2)k) +(k/\mu_0 h)\nu_1 2^{1-\nu_1}E_z(h, \varphi, nk). \quad (13)$$

We now choose φ such that $(r=h/2, \varphi)$ will coincide with an H_x or H_y node on the mesh. At these nodes H_φ equals the relevant Cartesian component of $\boldsymbol{H}$ (or its opposite). Using the fact that $E_z=0$ at $r=0$ we observe that (13) has the same form as (5a) or (5b) except for a factor $C_S=\nu_1 2^{1-\nu_1}$. Consequently, the singularity at a corner can be taken into account by inserting this factor in (5a) and (5b). Since, for $\alpha \leqslant \pi$, we have $2^{-1/2} \leqslant C_S \leqslant 1$ no difficulties with the stability of the difference scheme have to be expected and indeed no instabilities due to the use of this factor have been observed. An analysis of (13) yields that it has a truncation error of the order $\nu_2 - 1$ in the space variables and of the second order in the time variable. A higher order accurate, but more complicated, approximation of the field near the edge can be obtained by taking into account the first two terms of (9) and (10).

B. Edge Singularities, H-Polarization

In the case of H-polarization C' passes through H_z-nodes. From (2) and (3) it follows that we have the boundary condition $\partial_n H_z=0$ on C'. For the nodes on a straight section of C' this boundary condition can easily be implemented. When the node is on the edge of a corner the situation is more complicated since (a) $\boldsymbol{n}$ is not defined at this node, and (b) H_z is not differentiable near this edge. As above we analyze the field near the edge by introducing a local polar coordinate system. In polar coordinates the field-equations read

$$\epsilon_0 \partial_t E_r = (1/r)\partial_\varphi H_z \tag{14a}$$

$$\epsilon_0 \partial_t E_\varphi = -\partial_r H_z \tag{14b}$$

$$\mu_0 \partial_t H_z = -(1/r)\big(\partial_r(rE_\varphi) - \partial_\varphi E_r\big). \tag{14c}$$

Near the edge, H_z, E_r, and E_φ can, by using the expansion given by Jones [8], be approximated as

$$H_z = c_0(t) + c_1(t) r^{\nu_1}\cos(\nu_1\varphi) + \cdots \tag{15}$$

$$E_r = c_1(t) Z_1^{(1)}(t)\sin(\nu_1\varphi) + \cdots \tag{16}$$

$$E_\varphi = c_0(t) Z_0^{(2)}(t) r + c_1(t) Z_1^{(2)}(t) r^{\nu_1 - 1}\cos(\nu_1\varphi) + \cdots \tag{17}$$

with ν_n from (11). Starting with the approximation of H_z at the edge (see Fig. 3) we have from (15) $H_z(i,j)=c_0(t)$ and consequently $H_z(i,j)$ is coupled only to those terms in (16) and (17) that do not depend on φ. Hence we have from (14c) and (17)

$$\mu_0 \partial_t H_z(i,j) = -(1/r)\partial_r\big(rE_\varphi^{(0)}(r,t)\big) = -2c_0(t)Z_0^{(2)}(t) \tag{18}$$

where $E_\varphi^{(0)}(r,t)=c_0(t)Z_0^{(2)}(t)r$ denotes the term in the expansion (17) of E_φ that does not depend on φ. Assuming that $E_\varphi^{(0)}(r,t)$ can be obtained from the E_x and E_y nodes at a distance $h/2$ from the edge we can write (18) as

$$\mu_0 \partial_t H_z(i,j) = -4E_\varphi^{(0)}(h/2,t)/h. \tag{19}$$

In order to obtain $E_\varphi^{(0)}$ we first note that E_x and E_y are available at nodes at a distance of $h/2$ from the edge and that these Cartesian field components are equal to E_φ or its opposite. The relevant values of E_φ, however, will not be equal to $E_\varphi^{(0)}$ but will also contain the φ-dependent terms of (17). $E_\varphi^{(0)}$ is obtained from them by using weighting constants w_i that depend on the angle α and on the orientation of the wedge. They have to be chosen such that the contributions of all φ-dependent terms of (17) cancel. It can be shown that (19) can be written as

TABLE I
WEIGHTS FOR THE COMPUTATION OF $H_z^{n+1}(i,j)$ AT A CORNER

S_c	α	w_1	w_2	w_3	w_4
$x \le ih \cup y \ge jh$	$3\pi/2$	0	2	2	0
$x \le ih \cup (x-y) \le (i-j)h$	$5\pi/4$	0	4/3	8/3	0
$x \le ih$	π	1	1	2	0
$(x-y) \le (i-j)h$	π	0	2	2	0
$x \le ih \cap (x-y) \le (i-j)h$	$3\pi/4$	4/5	8/5	8/5	0
$x \le ih \cap y \ge jh$	$\pi/2$	2/3	4/3	4/3	2/3
$(x-y) \le (i-j)h \cap (x+y) \le (i+j)h$	$\pi/2$	4/3	4/3	4/3	0
$(x+y) \le (i+j)h \cap y \ge jh$	$\pi/4$	8/7	8/7	8/7	4/7
$(x+y) = (i+j)h \cap x \le ih$	0	1	1	1	1
$y = jh \cap x \le ih$	0	1	1	1	1/2*

*$E_x^{n+\frac{1}{2}}(i-1/2,j)$ has a value on both sides of S_c, each of which has to be taken into account with a weight 1/2.

$$\begin{aligned} H_z^{n+1}(i,j) = {} & H_z^n(i,j) + (k/\mu_0 h) \\ & \cdot\big(w_1 E_x^{n+1/2}(i,j+1/2) \\ & - w_2 E_x^{n+1/2}(i,j-1/2) \\ & - w_3 E_y^{n+1/2}(i+1/2,j) \\ & + w_y E_y^{n+1/2}(i-1/2,j)\big). \end{aligned} \tag{20}$$

In Table I the weights are given for a number of angles α and for certain orientations of the wedge. All other configurations with a corner that can occur under the assumptions we have made regarding the boundary C' (see Section II) can be dealt with using the weights given in Table I and symmetry properties. Equation (20) has the same form as the finite-difference approximation of (2c) in a domain with discontinuities in the permittivity. For completeness we have added the case $\alpha=\pi$ (i.e., a plane boundary) to Table I.

Having found an approximation for H_z at the edge of a corner we now start with the derivation of equations that apply to the E_x and E_y nodes at a distance $h/2$ from the edge. Applying (14a) to a point with $r=h/2$ and using the first two terms of (15) we obtain, after some manipulations

$$\begin{aligned} \epsilon_0 \partial_t E_\varphi(h/2,\varphi,t) &= -\big(\partial_r H_z(r,\varphi,t)\big)\big|_{r=h/2} \\ &= -\nu_1 2^{1-\nu_1}\big(H_z(h,\varphi,t) - H_z(0,\varphi,t)\big)/h \end{aligned} \tag{21}$$

where we have used the fact that the first term in (15) does not depend on r. Using the central difference approximation for the time derivative we obtain from (21)

$$\begin{aligned} E_\varphi(h/2,\varphi,(n+1/2)k) = {} & E_\varphi(h/2,\varphi,(n-1/2)k) \\ & - (k/\epsilon_0 h)\nu_1 2^{1-\nu_1}\big(H_z(h,\varphi,nk) - H_z(0,\varphi,nk)\big). \end{aligned} \tag{22}$$

We now choose φ such that $(r=h/2,\varphi)$ coincides with an E_x or E_y node on the mesh. At these nodes E_φ equals the relevant Cartesian component of $\boldsymbol{E}$, or its opposite, and we see that (22) has the same form as (6a) or (6b) except for a factor $C_S=\nu_1 2^{1-\nu_1}$, which can easily be inserted in for them to account for the edge singularities. As in the case of E-polarization no instabilities due to the modelling of the edge singularities have to be expected and no instabilities due to the use of this factor have been observed. An analysis of (20) and (22) reveals that the local truncation error near the edge is of the order ν_2-1 in the space variables and of the second order in the time variable. A higher order accurate approximation of the field near the edge can be obtained by taking into account the first three terms of (15) and (17).

IV. Numerical Results

In this section we shall demonstrate the accuracy and the improvement in the rate of convergence that is achieved by using our approximations for the edge singularities. We compare results that have been obtained by using our approximations near the edge with those obtained when the singularity was not taken into account. Since it is easier to make such a comparison for E-polarization than for H-polarization we will give results for the former case only. The fields in the configuration are caused by a time harmonic incident plane wave

$$E_z=\sin\left(2\pi(x+c_0t)/\lambda\right)\epsilon(x+c_0t) \tag{23}$$

propagating in the direction of decreasing x (see Fig 4) and having a wavelength λ. In (23) $\epsilon(x)$ denotes the Heaviside unit step function. The wavefront of the incident field arrives at $t=0$ at the left-hand side of the square finite-difference mesh of size $0.8\ \lambda*0.8\lambda$. The computations are carried out for a conducting obstacle S having an edge at the center of the mesh. The obstacle is assumed to be surrounded by a vacuum and we have used highly absorbing boundary conditions [9] at the boundaries of the mesh to simulate the relevant unbounded environment. We have used the maximum time step that is admissible for stability (7), and the results are presented for $t=1.5\lambda/(c_0\sqrt{2})$. In Fig. 4 the electric field near the edge is plotted for an edge with $\alpha=0$ and, in order to study convergence, for $h=\lambda/10$, $\lambda/20$, and $\lambda/40$.

From this figure we observe that when the singularity is not taken into account the results are inaccurate and converge very slowly as $h\to 0$. When the singularity is taken into account convergence is much faster and accurate results are already obtained for $n=\lambda/h=20$. In Table II we present some numerical results to further show the improvement that is obtained by accounting for the singularities. To this aim we observe that, in general, the most refined mesh leads to the best results. Comparing now, for each included angle, the two columns we see that even for a coarse mesh inclusion of the singularity gives already good results. Of course a further improvement is obtained upon refining the mesh.

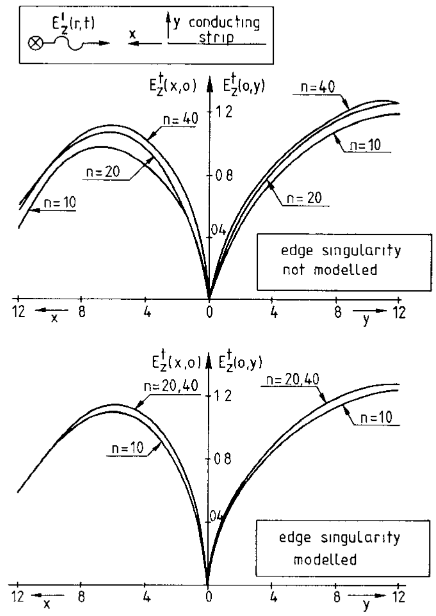

Fig. 4. Comparison of results for the field near the edge of a perfectly conducting strip computed with and without taking into account the singularity near the edge ($n=\lambda/h$).

TABLE II
Comparison of Results for $E_z(4,0)$

α \ n	0		π/4		π/2		3π/4	
	sing. incl.		sing. incl.		sing. incl.		sing. incl.	
	no	yes	no	yes	no	yes	no	yes
10	0.866	1.03	0.875	1.01	0.730	0.818	1.07	1.12
20	0.992	1.08	0.998	1.06	0.777	0.812	1.10	1.11
40	1.04	1.08	1.04	1.06	0.803	0.816	1.11	1.12

For each α results are given that are obtained accounting for the singularity (yes) (i.e. by using equation (13)) and without accounting for the singularity (no).

We observe that the necessity of taking into account the singularity increases with decreasing α, which is to be expected since the order of the singularity increases with decreasing α. Numerical experience in the case of H-polarization shows that, when the singularity is taken into account, the same accuracy and convergence is obtained as in the case of E-polarization.

V. Conclusion

In this paper we have shown that when the time-domain electromagnetic-field equations are solved by using a finite-difference technique singularities in the field due to a corner can, and should be, taken into account. We have described a very simple and stable method to do this. Our method retains the simplicity of the finite-difference method since its implementation only requires the adjustment of a few constants in the finite-difference equations that are used near the edge of a corner.

Acknowledgment

The research presented in this paper was carried out when the author was staying at the Department of Electrical and Electronic Engineering, University of Nottingham, U.K., with the financial support of a fellowship from the Royal Society.

References

[1] K. S. Yee, "Numerical solution of initial boundary value problems involving Maxwell's equations in isotropic media," *IEEE Trans. Antennas Propagat.*, vol. AP-14, pp. 302–307, May 1966.

[2] C. D. Taylor, D.-H. Lam, and T. H. Shumpert, "Electromagnetic pulse scattering in time-varying inhomogeneous media," *IEEE Trans. Antennas Propagat.*, vol. AP-17, pp. 585–589, Sept. 1969.

[3] A. Taflove and M. E. Brodwin, "Numerical solution of steady-state electromagnetic scattering problems using the time dependent Maxwell's equations," *IEEE Trans. Microwave Theory Tech.*, vol. MTT-23, pp. 623–630, Aug. 1975.

[4] D. E. Merewether, "Transient currents induced on a metallic body of revolution by an electromagnetic pulse," *IEEE Trans. Electromagn. Compat.*, vol. EMC-13, pp. 41–44, May 1971.

[5] K. S. Kunz and K.-M. Lee, "A three-dimensional finite-difference solution of the external response of an aircraft to a complex transient EM environment: Part I—The method and its implementation." *IEEE Trans. Electromagn. Compat.*, vol. EMC-20, pp. 328–333, May 1978.

[6] A. Taflove, "Application of the finite-difference time-domain method to sinusoidal steady-state electromagnetic penetration problems," *IEEE Trans. Electromagn. Compat.*, vol. EMC-22, pp. 191–202, 1980.

[7] R. Holland, L. Simpson, and K. S. Kunz, "Finite-difference analysis of EMP coupling to lossy dielectric structures," *IEEE Trans. Electromagn. Compat.*, vol. EMC-22, pp. 203–209, 1980.

[8] D. S. Jones, *The Theory of Electromagnetism.* Oxford, England: Pergamon, 1964, p. 566.

[9] G. Mur, "Absorbing boundary conditions for the finite-difference approximation of the time-domain electromagnetic-field equations," submitted for publication.

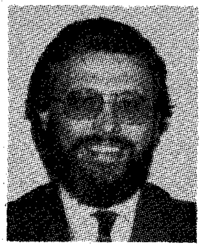

Gerrit Mur was born on February 16, 1942, in Laag-Nieuwkoop, the Netherlands. After graduating from a polytechnic in Utrecht in 1963 he obtained the masters degree in electrical engineering in 1970 and the Ph.D. degree in 1978, both from the Delft University of Technology, Delft, The Netherlands.

From 1970 he worked as a lecturer at the Department of Electrical Engineering of Delft University, and since 1978 he has been a Senior Lecturer. His main research interest is in the development and application of numerical methods for computing electromagnetic fields in complicated geometries.

Coupled-Mode Theory Analysis of Distributed Nonreciprocal Structures

IKUO AWAI, MEMBER, IEEE, AND TATSUO ITOH, SENIOR MEMBER, IEEE

***Abstract*—A general coupled-mode theory is developed for dielectric waveguide structures containing a gyrotropic layer. The theory is applied to several specific structures. Based on qualitative and numerical analyses, we studied the feasibility of such structures as the new type of nonreciprocal devices for millimeter-wave applications. A number of considerations for practical designs are included.**

Manuscript received March 27, 1981; revised June 3, 1981. This work was supported by ONR under Contract N00014-C-0553 and in part under a Joint Services Electronics Program F49620-77-C-0101. The major portion of this paper was presented at the 1981 International Microwave Symposium.

I. Awai was with the Department of Electrical Engineering, University of Texas, Austin, TX 78712. He is now with the Department of Electronic Engineering, Kyoto University, Kyoto, Japan.

T. Itoh is with the Department of Electrical Engineering, University of Texas, Austin, TX 78712.

I. Introduction

DEVELOPMENT of microwave and millimeter-wave isolators and circulators becomes more difficult as the frequency is increased [1], [2]. This is because the nonreciprocal property of ferrite used for these devices represented by the ratio of off-diagonal and diagonal components of the permeability tensor decreases with the frequency. One solution is to use a ferrite with high-saturation magnetization ($4\pi M$). However, it is difficult to obtain a ferrite material with more than 5 kG of $4\pi M$.